Optical knife-edge displacement sensor for high-speed atomic force microscopy

Christoph Braunsmann,[1] Veronika Prucker,[2] and Tilman E. Schäffer[1,a)]
[1]*Institute of Applied Physics and LISA+, University of Tübingen, Auf der Morgenstelle 10, 72076 Tübingen, Germany*
[2]*Institute of Applied Physics, University of Erlangen-Nürnberg, Staudtstraße 7, 91058 Erlangen, Germany*

(Received 18 January 2014; accepted 22 February 2014; published online 10 March 2014)

We show that an optical knife-edge technique can be used to detect the parallel shift of an object with sub-nanometer resolution over a wide bandwidth. This allows to design simple, contact-free, and high-speed displacement sensors that can be implemented in high-speed atomic force microscope scanners. In an experimental setup, we achieved a root-mean-square sensor noise of 0.8 nm within a bandwidth from 1 Hz to 1.1 MHz. We used this sensor to detect and correct the nonlinear z-piezo displacement during force curves acquired with rates of up to 5 kHz. We discuss the fundamental resolution limit and the linearity of the sensor. © *2014 AIP Publishing LLC*. [http://dx.doi.org/10.1063/1.4868043]

High-speed atomic force microscopes (AFMs) provide up to 1000 times faster imaging speeds compared to conventional AFMs and allow the imaging of fast dynamic processes.[1–4] However, high-speed AFMs have not or only rarely been used for applications that require accurate and precise nanopositioning such as nanolithography,[5] force spectroscopy,[6,7] or nanoindentation. This is partially owing to the difficulty of correcting the motions of the piezoelectric actuators (piezos) in high-speed AFM scanners for nonlinearity, hysteresis, and creep. The x- and y-piezo hysteresis of high-speed scanners has been reduced by applying an open loop control method based on polynomial-approximations.[8] Strain gauges have been employed for linearizing the lateral high-speed scanner motion with an open loop iterative learning method.[9] Nevertheless, open loop methods cannot be used for non-periodic scanner motions and the noise level of strain gauges is often too high to detect fast scanner displacements with a sufficient bandwidth and (sub)nanometer resolution.[9,10] The induced charge of the piezo has been used as a measure of piezo displacement and allowed reducing piezo hysteresis over a wide bandwidth.[11] However, the proposed setup did not allow the measurement of low frequency or static piezo displacements.

We present a displacement sensor that is well-suited to fulfill the requirements of high-speed AFMs: (i) The sensor size must be small to be compatible with the small size of high-speed scanners. (ii) The sensor bandwidth should be above 100 kHz and its resolution on the nanometer scale to accurately detect the high-speed scanner motions, especially in the fast z-direction. (iii) The mass of the sensor component that is physically attached to the scanner should be small to maintain the high resonant frequencies of the scanner. Our sensor is based on an optical knife-edge technique, providing contact-free displacement sensing with high resolution and a large bandwidth. Knife-edge techniques are commonly used for optical beam profiling of laser beams.[12] They have also been applied to measure the displacement of cantilever beams in acoustic atomic force microscopy[13] and doubly clamped beams in nanoelectromechanical systems.[14]

The sensor was implemented in a high-speed AFM scanner and measured the z-displacement of the z-piezo and an attached sample stage [Fig. 1(a)]. The collimated beam from a laser diode with an elliptical Gaussian intensity distribution was passed through a focusing lens, was reflected from a small mirror glued to the sample stage, and was focused onto a knife-edge. The knife-edge was attached to a tilt-stage (not shown in Fig. 1), which allowed us to center the laser spot on the knife-edge before the experiment so that 50% of the total power of the laser beam was transmitted onto the photodiode. A z-displacement of the z-piezo caused a parallel shift of the reflected beam, $s = 2z\cos\alpha$, where α was the incident angle of the beam [Fig. 1(b)]. The resulting shift s of the laser spot on the knife-edge [Fig. 1(c)] caused a change in the transmitted laser power, which was measured by the photodiode and provided the output signal of the sensor. Note that the principle of our sensor is different from optical lever systems, where a changing reflection angle (a surface tilt) instead of a parallel shift of a surface is measured. Additionally, in an optical lever system the laser is typically focused on the object to be measured (e.g., a cantilever) and not on the detector as in the knife-edge sensor. As mirror we used a thin circular disc of freshly cleaved mica that was coated with gold (radius 2.3 mm). The mass of this small mirror was negligible compared to the mass of the z-piezo and sample stage and therefore did not significantly reduce its resonant frequencies (fundamental z-resonance at ≈37 kHz). In our setup the mirror was fixed beneath the sample stage, but it could be placed at any location that displaces in parallel with the sample. The diffraction at the knife-edge causes the transmitted beam to spread. The photodiode should therefore be placed directly behind the knife-edge to detect the full transmitted laser power. For this reason, we found that mounting the knife-edge at the z-piezo[15] and thus displacing the knife-edge instead of using a mirror is not feasible owing to space constraints imposed by the sample stage and the cantilever holder.

The one-dimensional irradiance distribution of the laser spot on the knife-edge in the ξ-direction is given by

a)Author to whom correspondence should be addressed. Electronic mail: tilman.schaeffer@uni-tuebingen.de.

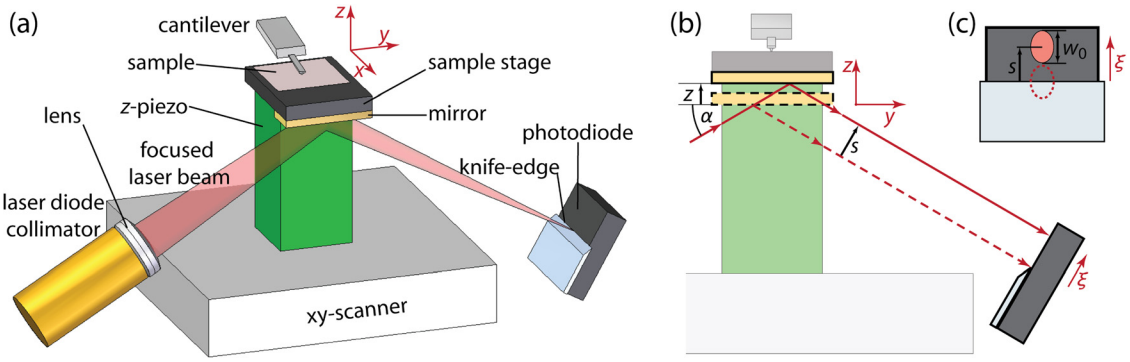

FIG. 1. (a) Functional principle of the optical knife-edge displacement sensor. The sensor detects the parallel shift of a laser beam that is reflected from an ultra-light mirror attached to the sample stage and focused onto a knife-edge located in front of a photodiode. (b) Axis of the laser beam before (dashed red line) and after (solid red line) a z-piezo displacement. The z-displacement causes a parallel shift s of the beam. (c) Shift s of the focused spot (red disc) on the knife-edge. The $1/e^2$ diameter of the spot in the ξ-direction is w_0. To illustrate the principle of the sensor more clearly, the z-piezo displacement, the parallel shift s, and the dimensions of the laser spot were drawn highly exaggerated.

$$I(\xi) = \sqrt{\frac{8}{\pi}}\frac{P_{\text{tot}}}{w_0}\exp\left(-\frac{8(\xi - s)^2}{w_0^2}\right), \tag{1}$$

where w_0 is the $1/e^2$ diameter of the focused spot and P_{tot} is the total power of the laser beam. If the full laser power transmitted by the knife-edge is detected by the photodiode, the sensor signal [Fig. 2, red curve] becomes

$$P(s) = \int_0^{+\infty} I(\xi)d\xi = \frac{1}{2}P_{\text{tot}}\left[1 + \text{erf}\left(\frac{\sqrt{8}s}{w_0}\right)\right]. \tag{2}$$

The sensor sensitivity (= the slope dP/ds of the sensor signal) is maximal at $s = 0$ and gradually decreases toward zero when the spot shifts away from the center of the knife-edge. For spot shifts that are small compared to w_0 the sensor signal changes linearly with s

$$P_{\text{lin}}(s) = \frac{1}{2}P_{\text{tot}} + \sqrt{\frac{8}{\pi}}\frac{P_{\text{tot}}}{w_0}s. \tag{3}$$

The nonlinearity of the sensor signal can be defined as the relative deviation between the sensor signal Eq. (2) and the linear approximation Eq. (3) [Fig. 2, blue curve]. The nonlinearity is below $\pm 0.1\%$ within an s-range of $\pm 0.06\ w_0$ and below $\pm 1\%$ within an s-range of $\pm 0.13\ w_0$.

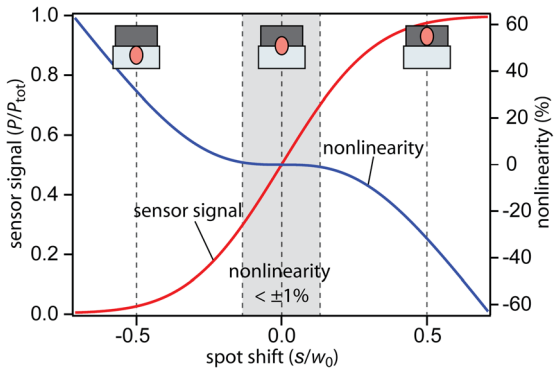

FIG. 2. Sensor signal and sensor nonlinearity calculated as a function of the spot shift s relative to the spot diameter w_0. The corresponding z-displacement is $z = s/(2\cos\alpha)$. The three insets show the positions of the Gaussian laser spot on the knife-edge for a spot shift s of $-w_0/2$, 0, and $w_0/2$, respectively.

The fundamental detection limit of the knife-edge sensor is determined by the photonic shot noise, which arises from photon counting described by Poisson statistics and whose root-mean-square (rms) value is given by[16]

$$\Delta P = \sqrt{2\frac{hc}{\lambda}P_{\text{lin}}(0)\Delta f} = \sqrt{\frac{hc}{\lambda}P_{\text{tot}}\ \Delta f}\,, \tag{4}$$

where h is Planck's constant, c the velocity of light, λ the laser wavelength, and Δf the detection bandwidth. We assumed that the sensor works in its linear range around $s = 0$. Using the sensor sensitivity $dP_{lin}/ds = \sqrt{8/\pi}P_{tot}/w_0$ and $z = s/(2\cos\alpha)$ gives the rms shot noise

$$\Delta z = \sqrt{\frac{\pi hc}{32\,\lambda\,P_{\text{tot}}}\Delta f}\ \frac{w_0}{\cos\alpha}\,. \tag{5}$$

The minimum detectable displacement z_{min} is obtained at a signal-to-noise ratio of 1, giving $z_{\text{min}} = \Delta z$. In principle, z_{min} can be reduced by decreasing the spot diameter w_0. However, decreasing w_0 also decreases the linear detection range (e.g., the z-range that provides a nonlinearity $< \pm 0.1\%$) by the same ratio. The spot diameter should thus be adapted to the maximum displacement to be measured. Using the parameters from our setup ($w_0 = 49\ \mu$m, $\lambda = 670$ nm, $\alpha = 45°$, and $P_{\text{tot}} = 5$ mW) gives a shot noise level of $\Delta z/\sqrt{\Delta f} = 0.17\ \text{pm}/\sqrt{\text{Hz}}$. The linear detection range (for a nonlinearity $< \pm 0.1\%$) was $\pm 2.2\ \mu$m, which is larger than the maximum range of our z-piezo ($\pm 2\ \mu$m).

In practice, the measured noise level (2.8 $\text{pm}/\sqrt{\text{Hz}}$ at 1 kHz) was larger than the theoretical limit owing to laser intensity fluctuations, which showed a $1/f$ -like behavior for frequencies below 1 kHz and a roll-off for frequencies above 10 kHz. The rms noise measured in between 1 Hz and 1.1 MHz was 0.8 nm. The low-frequency sensor drift was below 50 nm within 30 min. The measured sensor nonlinearity was $< \pm 0.6\%$, which is also larger than the theoretical limit ($< \pm 0.1\%$). This deviation may partially be explained by the finite roughness of the used knife-edge (the edge of a scalpel blade).

We used the optical knife-edge sensor to detect the z-piezo displacement during force curves recorded on a mica surface in air at different rates (Fig. 3). The cantilever

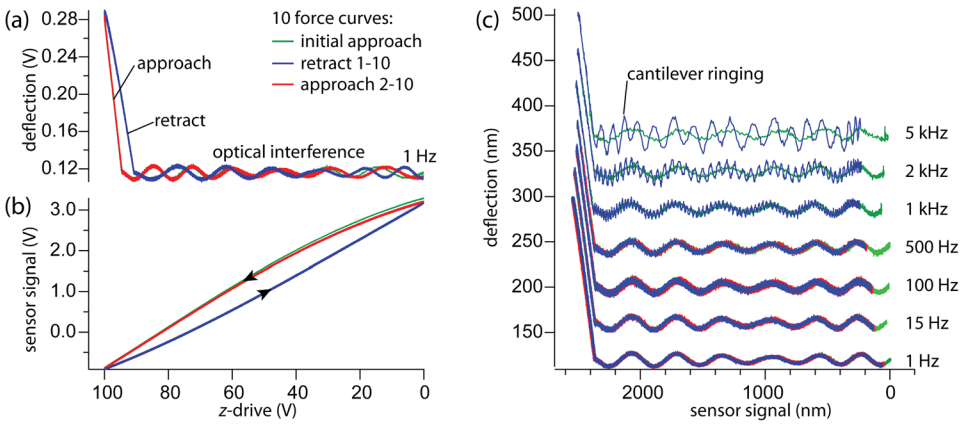

FIG. 3. (a) Cantilever deflection plotted against the z-drive voltage for 10 force curves recorded on mica in air (1 Hz force curve rate). The approach (green, red) and retract curves (blue) do not overlap owing to z-piezo hysteresis. To reveal the z-piezo hysteresis in the non-contact part (drive voltages $<\approx$90 V) of the force curve, a modulation of the deflection was purposefully induced using optical interference. The initial approach curve (green) does not overlap with the subsequent approach curves (red) due to z-piezo creep. (b) Simultaneously recorded sensor signal, showing piezo hysteresis and creep. (c) High-speed force curves (deflection versus sensor signal calibrated in nanometer). The bottom curve (1 Hz force curve rate) shows the data from (a) and (b). The approach and retract parts perfectly overlap, showing that the sensor accurately corrects for piezo hysteresis and creep. The correction also works for higher force curve rates (upper curves). At a rate of $\approx$1 kHz and above, the resonant ringing of the AFM cantilever becomes visible as high-frequency oscillations, which are superimposed on the optical interference pattern. For these force curves, just the initial approach and the first retract parts are shown for clarity.

deflection was detected by a homebuilt, high-speed AFM head. A sinusoidal drive voltage with a peak-to-peak amplitude of 100 V was applied to the z-piezo, and ten consecutive force curves with a rate of 1 Hz were recorded [Fig. 3(a)]. The deflection increased steeply for drive voltages $>\approx$90 V, indicating that the cantilever tip was in contact with the surface. In the non-contact part (z-drive $<\approx$90 V), the measured deflection was constant on average but was superimposed by a modulation owing to optical interference. This interference was purposefully induced by positioning the laser spot in the AFM head at the edge of the cantilever. The resulting modulation of the deflection, which is usually unwanted, served us as a built-in ruler to calibrate the sensor signal in nanometers.[17] To allow for a more precise calibration using a larger and more regular modulation, we temporarily replaced the mica sample with a small mirror that had the same tilt as the AFM cantilever.

The approach (green, red) and retract curves (blue) were significantly mismatched both in the contact and in the non-contact part [Fig. 3(a)]. The simultaneously recorded sensor signal [Fig. 3(b)] also showed a significant mismatch between the approach and retract curves, revealing the effect of z-piezo hysteresis (up to 14% relative to the signal range). The initial approach curve (green) did not overlap with the subsequent approach curves owing to z-piezo creep. When plotting the deflection from Fig. 3(a) versus the sensor signal from Fig. 3(b) [Fig. 3(c), bottom curve], the approach and the retract curves perfectly overlapped. The knife-edge sensor thus accurately corrected for piezo hysteresis and creep.

To demonstrate the high-speed abilities of the knife-edge sensor, we recorded force curves at high rates [Fig. 3(c)]. The force curves overlapped in their contact and non-contact parts and were identical among different rates. For rates of $\approx$1 kHz and above, a further periodic signal became visible (frequency $\approx$230 kHz). This corresponded to the resonant ringing of the AFM cantilever (PPP-NCH, NanoWorld, Neuchâtel). The amplitude of this ringing strongly increased with increasing force curve rate since the adhesion force, which caused the ringing, increased with the force curve velocity[7] [force curve velocities in Fig. 3(c) ranged from 4.6 μm/s to 2.3 cm/s]. For quantitative high-speed force curve measurements, it is therefore of advantage to use small cantilevers with high resonant frequencies and low quality factors,[18] which strongly reduces the decay time of cantilever resonances.

We applied the sensor to measure the mechanical properties of a silicone elastomer (Sylgard 184, Dow Corning, Midland, MI, USA) by recording high-speed force curves with a small cantilever (prototype, NanoWorld, Neuchâtel, Switzerland). The two components of the elastomer were thoroughly mixed in a 1:10 ratio, spread on a mica surface, and cured at room temperature for 48 h. The measurements were performed in distilled water to eliminate capillary forces. The viscous drag forces acting on the cantilever induced by the motion through the water were subtracted from the recorded force by assuming that the viscous drag is proportional to the cantilever tip velocity.[20,21] An analysis of the corrected force curves with Sneddon's contact model for conical tips[22] allowed calculating the apparent elastic modulus of the sample (see Ref. 23 for more details). We found that the apparent modulus increased with an almost constant slope when plotted on a log-log scale [Fig. 4, black triangles]. The apparent modulus increased from 2.5 $\pm$ 0.1 MPa at a force curve rate of 0.25 Hz to an apparent modulus of 5.2 $\pm$ 0.4 MPa at 3 kHz (average value $\pm$ standard deviation from ten force curves). This increase is explained by the viscoelastic nature of the elastomer. The shore hardness of 43 A (from the manufacturer's data sheet) can be converted to an elastic modulus of $\approx$2.5 MPa.[24] This compares well with the measured apparent modulus at 0.25 Hz, which is reasonable, because shore hardness measurements are usually performed on a time scale of seconds. Sneddon's contact model assumes a linear elastic sample and not a viscoelastic one. We therefore termed the calculated moduli "apparent moduli." The apparent moduli evaluated without the optical knife-edge sensor (just by using the drive voltage as it is common practice) were significantly larger by factors of 1.4 and 2.4 at rates of 0.25 Hz and 3.0 kHz, respectively [Fig. 4, open circles]. Piezo hysteresis and creep therefore have a

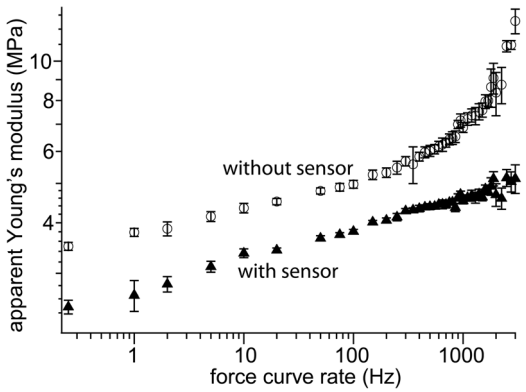

FIG. 4. Mechanical behavior of a silicone elastomer obtained by recording high-speed force curves with a small cantilever (z-distance = 1.3 μm, peak force ≈ 25 nN). The apparent Young's modulus was obtained by fitting Sneddon's contact model for conical tips to the approach part of the force curves. The data points and error bars correspond to the average value and standard deviation, respectively (10 force curves for each force curve rate). The apparent modulus increased when increasing the force curve rate from 0.25 Hz to 3 kHz. Using the true z-piezo displacement measured with the knife-edge sensor (black triangles) gave 1.4–2.4 times smaller apparent moduli than when doing the analysis without the sensor (open circles). The small cantilever had a rectangular shape (length 20 μm, width 7.5 μm, and thickness 0.5 μm), a conical tip (length 2.5 μm and half-cone angle 8°), and a spring constant of 1.3 N/m (calibrated with the thermal noise method[19]). The elastomer was assumed to be incompressible (Poisson's ratio $\nu = 0.5$).

significant influence on quantitative mechanical measurements and should be corrected by using a displacement sensor.

To conclude, we devised and analyzed a high-speed displacement sensor with sub-nanometer resolution, which can be easily implemented in scanners for high-speed atomic force microscopy. The space requirements of this simple, inexpensive, and contact-free sensor are low. The electronic bandwidth of the sensor is limited only by the bandwidth of the photodiode amplifier and can easily exceed 1 MHz. We showed that the optical knife-edge sensor can measure the true z-piezo displacement while recording force curves with kHz-rates, which allowed for quantitative high-speed measurements of mechanical sample properties. This paper focused on the application to high-speed atomic force microscopy, but the knife-edge sensor may be used in many other applications where high-speed displacement sensing with sub-nanometer resolution is required.

The authors thank Alexander Tobisch for constructing the AFM head, Stefan Ballmann for coating the mica mirrors with gold, Johannes Rheinlaender for helpful discussions, and NanoWorld for providing the small cantilever. This work was financially supported by the BMBF (Grant No. 13N12162).

[1]S. R. Manalis, S. C. Minne, A. Atalar, and C. F. Quate, Rev. Sci. Instrum. **67**(9), 3294–3297 (1996).
[2]T. Ando, N. Kodera, E. Takai, D. Maruyama, K. Saito, and A. Toda, Proc. Natl. Acad. Sci. U.S.A. **98**, 12468–12472 (2001).
[3]J. H. Kindt, G. E. Fantner, J. A. Cutroni, and P. K. Hansma, Ultramicroscopy **100**, 259–265 (2004).
[4]C. Braunsmann and T. E. Schäffer, Nanotechnology **21**(22), 225705 (2010).
[5]P. C. Paul, A. W. Knoll, F. Holzner, M. Despont, and U. Duerig, Nanotechnology **22**(27), 275306 (2011).
[6]M. B. Viani, T. E. Schäffer, A. Chand, M. Rief, H. E. Gaub, and P. K. Hansma, J. Appl. Phys. **86**(4), 2258–2262 (1999).
[7]A. Ptak, M. Kappl, and H. J. Butt, Appl. Phys. Lett. **88**(26), 263109 (2006).
[8]H. Watanabe, T. Uchihashi, T. Kobashi, M. Shibata, J. Nishiyama, R. Yasuda, and T. Ando, Rev. Sci. Instrum. **84**(5), 053702 (2013).
[9]G. Schitter, Tech. Mess. **76**(5), 266–273 (2009).
[10]A. J. Fleming and K. L. Leang, Sens. Actuators A **161**, 256–265 (2010).
[11]M. Kageshima, S. Togo, Y. J. Li, Y. Naitoh, and Y. Sugawara, Rev. Sci. Instrum. **77**(10), 103701 (2006).
[12]J. A. Arnaud, W. M. Hubbard, G. D. Mandeville, B. de la Clavière, E. A. Franke, and J. M. Franke, Appl. Opt. **10**(12), 2775–2776 (1971).
[13]U. Rabe and W. Arnold, Appl. Phys. Lett. **64**(12), 1493–1495 (1994).
[14]D. Karabacak, T. Kouh, C. C. Huang, and K. L. Ekinci, Appl. Phys. Lett. **88**(19), 193122 (2006).
[15]G. Schitter, R. W. Stark, and A. Stemmer, Meas. Sci. Technol. **13**, N47–N48 (2002).
[16]T. E. Schäffer, J. Appl. Phys. **91**(7), 4739–4746 (2002).
[17]M. Jaschke and H. J. Butt, Rev. Sci. Instrum. **66**(2), 1258–1259 (1995).
[18]D. A. Walters, J. P. Cleveland, N. H. Thomson, P. K. Hansma, M. A. Wendman, G. Gurley, and V. Elings, Rev. Sci. Instrum. **67**(10), 3583–3590 (1996).
[19]S. M. Cook, T. E. Schäffer, K. M. Chynoweth, M. Wigton, R. W. Simmonds, and K. M. Lang, Nanotechnology **17**(9), 2135–2145 (2006).
[20]O. Marti, M. Holzwarth, and M. Beil, Nanotechnology **19**(38), 384015 (2008).
[21]R. E. Mahaffy, C. K. Shih, F. C. MacKintosh, and J. Käs, Phys. Rev. Lett. **85**(4), 880–883 (2000).
[22]I. N. Sneddon, Int. J. Eng. Sci. **3**(1), 47–57 (1965).
[23]Y. Jiao and T. E. Schäffer, Langmuir **20**(23), 10038–10045 (2004).
[24]A. W. Mix and A. J. Giacomin, J. Test. Eval. **39**(4), 696–705 (2011).